Vibrational Modes of the Vinyl and Deuterated Vinyl Radicals

Matthew Nikow,[†] Michael J. Wilhelm,[†] and Hai-Lung Dai*[,‡]

Department of Chemistry, University of Pennsylvania, Philadelphia, Pennsylvania 19104, and Department of Chemistry, Temple University, Philadelphia, Pennsylvania 19122

Received: November 4, 2008; Revised Manuscript Received: June 22, 2009

Following the initial report of the detection of fundamental transitions of all nine vibrational modes of the vinyl radical [Letendre, L.; Liu, D.-K.; Pibel, C. D.; Halpern, J. B.; Dai, H.-L. *J. Chem. Phys.* **2000**, *112*, 9209] by time-resolved IR emission spectroscopy, we have re-examined the assignments of the vibrational modes through isotope substitution. Precursor molecules vinyl chloride-d_3, vinyl bromide-d_3, and 1,3-butadiene-d_6 are used for generating vibrationally excited vinyl-d_3 through 193 nm photolysis. The nondeuterated versions of these molecules along with vinyl iodide and methyl vinyl ketone are used as precursors for the production of vinyl-h_3. IR emission following the 193 nm photolysis laser pulse is recorded with nanosecond time and ~8 cm^{-1} frequency resolution. A room-temperature acetylene gas cell is used as a filter to remove the fundamental transitions of acetylene, a photolysis product, in order to reduce the complexity of the emission spectra. Two-dimensional cross-spectra correlation analysis is used to identify the emission bands from the same emitting species and improve the *S/N* of the emission spectra. Isotope substitution allows the identification of several low-frequency vibrational modes. For C_2H_3, the assigned modes are the ν_4 (CC stretch) at 1595, ν_5 (CH_2 symmetric bend) at 1401, ν_6 (CH_2 asymmetric + α-CH bend) at 1074, ν_8 (CH_2 + α-CH symmetric out-of-plane (oop) bend) at 944, and ν_9 (CH_2 + α-CH asymmetric oop bend) at 897 cm^{-1}. For C_2D_3, the modes are the ν_5 (CD_2 symmetric bend) at 1060, ν_6 (CD_2 asymmetric + α-CD bend) at 820, and ν_8 (CD_2 + α-CD symmetric oop bend) at 728 cm^{-1}.

I. Introduction

Vinyl radicals in both the condensed and gas phases have been of critical importance in reaction pathways as intermediates in reactions involving small organic molecules.[2] Such small olefinic molecules have also recently garnered much interest as models for larger, more complex systems of reactions.[3,4] On the other hand, radical species such as vinyl are often hard to characterize and identify due to their transient, short-lived nature as well as their low abundance. This is particularly true for the observation of these radicals through vibrational spectroscopy in the infrared (IR) region due to their small transition dipole moments for vibrational motions.

In contrast to the wealth of information on the excited electronic states[5−15] as well as the production of the vinyl radical,[16−32] there have been relatively fewer reports on the vibrational modes of the ground state of the vinyl radical.[33−35] Kanamori et al.[33] first detected one pure c-type band, the ν_9 mode, at 895 cm^{-1} by IR diode laser kinetic spectroscopy and determined the barrier height of the double minimum potential of the α-C−H in-plane oscillation. There has also been work done on ground-state vinyl in noble gas matrixes.[36−39] Shepherd et al.[36] used carbon-13 and deuterium-substituted ethylene to generate vinyl radicals and reported an out-of-plane (oop) bending mode at 900 cm^{-1}, labeled the ν_7 band,[40] for C_2H_3 and the corresponding frequencies from six other isotopomers. Forney et al. also reported the observation of this band in matrixes.[39] A more recent work by Tanskanen et al.[37] identified the ν_5 and ν_7 bending modes[40] for six isotopomers, including C_2H_3 and C_2D_3, of the vinyl radical in noble gas matrixes. The vinyl produced was generated from the photolysis of acetylene and annealing of the matrix to mobilize hydrogen atoms. In these prior matrix works, the observed mode was incorrectly assigned to ν_7, which is the lowest-energy in-plane (ip) bending mode. It is now correctly labeled as ν_9, the lowest-energy oop bending mode. The most recent work on the IR signature of the vinyl radical was done by using a synchrotron to irradiate ethylene in solid Ne at 3 K.[41] Wu and co-workers found seven of the nine modes of the $^{12}C_2H_3$ and $^{13}C_2H_3$ radicals and six of the nine modes of the C_2D_3 radical.

Time-resolved Fourier transform IR emission spectroscopy[42−45] (TR-FTIRES) has been applied for the spectroscopic identification of the vibrational modes of several transient radicals, including vinyl,[1] cyanovinyl,[46] HCCO,[47] and OCCN.[46,48] In its first application, which resulted in the initial report[1] of all nine vibrational modes of the vinyl radical, four different precursor molecules were utilized to generate vibrationally hot vinyl radicals through UV laser photolysis. Vibrationally excited vinyl generated through precursor photolysis would emit IR photons through the IR-active modes which can be detected with time and frequency resolution in TR-FTIRES. The experiments were conducted with low-pressure (~10−100 mTorr) precursor gas mixed in with >4 Torr of Ar buffer gas. Collision with the buffer gas renders less vibrational energy in vinyl. Eventually, the IR emission at longer time (10−100 μs) represents the fundamental transitions of the IR-active modes. Assignment of the IR emission bands detected in the experiments to the vinyl radical was accomplished through comparison with theoretical calculations and prior studies and comparison among observations made with the different precursors.

Of the four precursor molecules used in the initial report on the vinyl radical,[1] vinyl bromide and vinyl chloride photolysis yielded significant amounts of vibrationally hot acetylene and

* To whom correspondence should be addressed. E-mail: hldai@temple.edu.
† University of Pennsylvania.
‡ Temple University.

10.1021/jp809735e CCC: $40.75 © 2009 American Chemical Society
Published on Web 07/13/2009

other fragments such as HBr/HCl, in addition to vinyl. The 1,3-butadiene precursor also generated some hot acetylene and other unidentifiable fragments in the photolysis reaction. Methyl vinyl ketone was previously determined to yield vinyl, methyl, and CO with unity quantum yield[18] and no other byproducts. In each of the four cases, a strong band at 1277 cm^{-1} was detected. This band was assigned to the ν_5 CH_2 symmetric bend mode. This assignment caused notable problems in comparison with previous theoretical calculations,[49−53] which otherwise have produced both frequencies and intensities in good agreement with experiments for all other modes.

Most recently, Sattelmeyer and Schaefer,[54] using the equation-of-motion coupled cluster theory for ionized states from the anion, calculated the intensity and harmonic frequency of the vinyl vibrational modes with the best theoretical precision. It was found that the ν_5 mode is calculated to be at 1419 cm^{-1}, still much to the blue of the reported 1277 cm^{-1}, with a significantly smaller intensity than that in the previous experimental report.[1] This comparison with theoretical calculations called for further examination of the original assignment of the experimentally detected IR emission bands, in particular, the one for the ν_5 mode.

It should be mentioned that even though the originally assigned higher-frequency CH stretching modes are in much better agreement with theoretical calculations, a recent experimental[55] work by Nesbitt and co-workers using high-resolution IR laser absorption of a slit-jet cooled sample following photolysis has found the strongest CH_2 symmetric stretching band at 2901 cm^{-1}, much to the red of the originally reported value[1] and the best theoretical harmonic calculation.[54]

In this work, in order to verify the assignment of the previously detected IR emission bands of vinyl, isotopic substitution of three precursors of the vinyl radical and an additional precursor molecule are used. A total of five molecules, vinyl bromide (VBr), vinyl chloride (VCl), vinyl iodide (VI), 1,3-butadiene (13BD), and methyl vinyl ketone (MVK), and three of their completely deuterated analogues, VBr-d_3, VCl-d_3, and 13BD-d_6 are used as precursors for generating vinyl or deuterated vinyl through photolysis at 193 nm.

Two-dimensional cross-spectral correlation (2DCSC) has been developed for deciphering spectral features from different spectra but belonging to the same species.[56] Correlations between spectral features are made based on their frequency and intensity temporal dependence in the time-resolved spectra. The set of emission spectral bands from the same species should share a similar time dependence and show positive correlation. Through the application of this method, we should be able to identify the emission features from vinyl and enhance their signal to noise (S/N) ratio in the spectra obtained from the five precursor molecules.

In order to ensure that the assignment of the emission features to the vinyl radical are not affected by the appearance of emission bands from vibrationally hot acetylene which may be in overlap with the vinyl bands, an IR filter containing room-temperature acetylene gas is used to remove fundamental emission from acetylene though absorption. The filter will selectively eliminate emission within the acetylene rovibrational absorption $v = 1 \leftarrow v = 0$ transitions. This filter is not effective for emission from highly vibrationally excited acetylene. However, as collisions render all excited species to lower energies and emission closer to the fundamental transitions, the acetylene filter can then more effectively remove the acetylene fundamental emission features from the latter-time emission spectra.

The cold chemical filtering experiment reveals that vibrationally hot acetylene is a major product in the photolysis reactions performed. Several emission features can be attributed to vibrationally hot acetylene. Modeling of these features[57] and extraction of the dynamics of highly vibrationally excited acetylene can be used as a starting point to study other acetylenic systems of interest including structural changes, energy transfer, and chemical reaction.[58−61]

In this report, we confirm, with better determined frequency, the assignment of four of the five bending modes and one stretching mode of the vinyl (C_2H_3) radical and three bending modes of the deuterated vinyl (C_2D_3) radical. The bending mode, ν_5, is assigned to a band much weaker than the originally assigned, strong band. The new results agree well with recent experimental results and theoretical calculations.

II. Experimental Section

The experimental setup has been previously described[42,43,45] and is briefly outlined here. The 193 nm pulses from an excimer laser (Lambda Physik, LPX200, 20 Hz, 10−50 mJ/pulse) were lightly focused into a gas cell with flowing precursor gas mixed in with a noble gas colliding partner. The precursors were vinyl bromide (Aldrich, >98%), vinyl chloride (Aldrich, 99.5%), 1,3-butadiene (Aldrich, >99%), vinyl iodide (Oakwood Products, 90%), or methyl vinyl ketone (Alfa Aesar, 90%). Deuterated precursor molecules included vinyl bromide-d_3 (CDN Isotopes, 99%), vinyl chloride-d_3 (Cambridge Isotopes, 98%), and 1,3-butadiene-d_6 (Cambridge Isotopes, 98%). All precursors were processed with at least one freeze−pump−thaw cycle to improve the purity and were examined through IR absorption spectroscopy analysis to ensure that no other detectable component was present. The colliding gas was typically Ar (Airgas, 99.999%) or He (Airgas, 99.999%). The precursor pressures were kept low (5−20 mTorr) as compared to the noble gas collider (2−8 Torr) to limit secondary reactions and allow quenching of the vibrationally excited molecules before exiting the IR collection area. A cold acetylene gas filter was constructed using a 15 cm long gas cell with KBr windows. The acetylene pressure inside of the cell was held between 1 and 10 Torr to provide substantial filtering of the acetylene bands. At a 4 Torr acetylene pressure, >90% filtering can be achieved for the moderately strong ν_3 CH stretch mode.

The emitted infrared radiation was collected by a set of 2 in. curved gold mirrors in a Welsh cell design. The IR emission from the Welsh cell was collected and collimated by a set of KCl lenses, with the focal length, *f*/4, of the last lens matched to the optics in the FTIR (Bruker IFS/66) housing a Michelson interferometer and detector (Judson, J15D14, MCT). A 4000 cm^{-1} low-pass filter was used to block high-frequency emission from folding into the spectra. The signal was amplified by an impedance-matched preamplifier (Judson, PA-101, DC) coupled to a wide bandwidth amplifier (Stanford Research, SR-445, 350 MHz, 500 Ω). The amplified signal was sent to a transient digitizer (Spectrum GMBH, PAD82a, 200 MHz, 8 bit) linked to the Opus (Bruker, v4.2) FTIR sampling program. Time-resolved step-scan slices were optically triggered and typically taken at 50 or 100 ns intervals with 4−12 cm^{-1} resolution.

III. Results

A. IR Emission Spectra Containing Vinyl-h_3 Features. The products and their energy content from the 193 nm photolysis of each of the five precursor molecules have been characterized via photofragment translational spectroscopy.[16,18−22] All five molecules with the exception of 1,3-butadiene generate

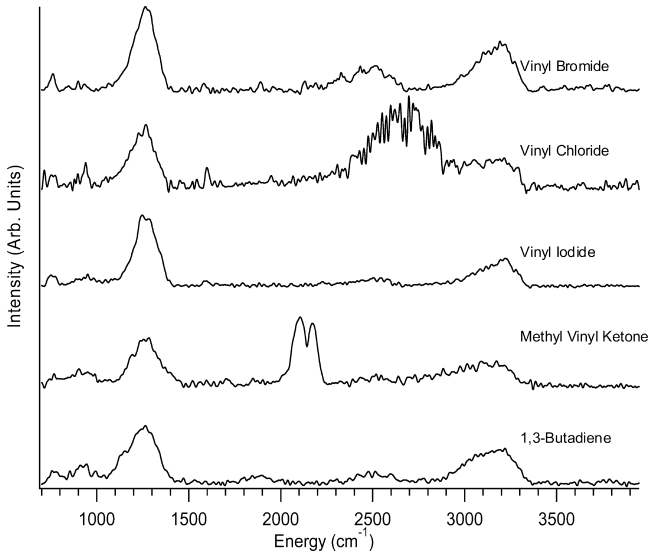

Figure 1. IR emission spectra recorded in between 2 and 3 μs following the photolysis of the five precursor molecules. Spectra are shown without correcting for the detector spectral response. No acetylene filter was used.

a significant quantity of the vinyl radical with acetylene as the other common product. Photolysis of 13BD yields a significant number of possible reaction channels, both molecular and radical, especially evident during the first several μs after photolysis.

The IR emission spectra following the photolysis of the five precursors, obtained without the use of the acetylene gas emission filter, are shown in Figure 1. Spectral features assigned to the vinyl radical are given in Table 1. The basis for the assignments will be given in the following sections. It should be noted that the relative intensities of the transitions shown in Figure 1 as well as subsequent spectra shown are emission intensities which have not been corrected for the experimental response function, and those reported in Table 1 are absorption intensities converted from emission intensities that have been corrected for the response function. In the following, the emission spectrum from each precursor is described separately first.

The time evolution of the reaction products of VBr is shown in Figure 2. Here, no acetylene filter was used to remove IR emission from the spectra. There are several low-energy features that decay rapidly after photolysis with little frequency shift. This is in marked contrast to the two main features at 1100−1400 and 3000−3300 cm^{-1}. These two features show a slow decay component as well as a large shift in frequency at early times. In the spectra detected following VBr and VCl photolysis, emissions from HBr and HCl appear, respectively, in each case between 2000 and 3000 cm^{-1}. Emission from the $v = 6$ HBr and the $v = 7$ HCl have been identified previously in the IR emission observed shortly after photolysis of VBr and VCl.[19,62,63] Accompanying this emission are two main features assignable to acetylene at 1300 and 3000−3300 cm^{-1}. Some additional low-energy emission bands also appear between 1000 cm^{-1} and the detector cutoff at around 700 cm^{-1}.

The photolysis of vinyl iodide has been well studied in the condensed phase[38,64] and in the gas phase.[17,65,66] At very low precursor pressures of a few mTorr, atomic iodine emission dominates the spectra. At higher pressures, the electronic transitions of iodine are quenched through collisions. Though some iodine emission bands are still apparent at 2500 cm^{-1}, under such experimental conditions, vinyl emission could also be detected. Emission assignable to acetylene is apparent in the spectra. HI, however, is not detected.

The dissociation of methyl vinyl ketone[18] leads primarily to methyl and vinyl radicals and CO in a sequential bond breaking mechanism. Emission from hot CO molecules is observed at around 2150 cm^{-1}. There may be some emission from methyl radicals, the deformation mode at 1400 cm^{-1} and the CH stretching modes at 3160 cm^{-1}, though these emission bands are masked by the unexpectedly strong emission features of acetylene following the MVK photolysis result as well.

IR emission following 1,3-butadiene photolysis can be complex as there are numerous available reaction channels available for generating molecular and radical products.[21] In addition to the main features attributed to acetylene, there is emission detected as a shoulder on the 1300 cm^{-1} feature. This shoulder may arise from a vibrationally excited radical other than vinyl as none of the other precursor photolysis results in emission in this region. There is also extra intensity found on the red side of the CH stretching feature that may also arise from vinyl or other radical products.

The strong feature at 1300 cm^{-1} and a part of the 3000−3300 cm^{-1} bands appearing in all spectra can be assigned to acetylene. The 1300 cm^{-1} feature was previously assigned to vinyl and has been an assignment of contention. This feature is now assigned to the unexpectedly strong $\nu_4 + \nu_5$ combination band. The basis of the assignment which involves substantial modeling of IR emission from vibrationally excited acetylene will appear elsewhere.[57] The same modeling also allows the assignment of part of the group of bands at 3000−3300 cm^{-1} to the acetylene ν_3 mode.

The time dependence of the emission features provides another consideration for their assignment. In general, primary photolysis reaction products peak within the first several μs, while secondary products and molecules excited though collision energy transfer appear later in the time-resolved spectra. The vinyl features are expected to peak at around 1 μs and decay with a much faster time constant due to reactions (with the exception in the 13BD case, where reactions lead to additional vinyl generation). In contrast, the acetylene emission features should show large anharmonic shifts due to high internal energy content. Its fundamental transitions may occur later (between 2 and 3 μs) and decay with a longer time constant.

Emission from secondary reaction products may become more prominent when the precursor pressure is increased since the amount of these reaction products increases nonlinearly with the pressure. Secondary product emission features also show a characteristic slower rise in time. It has been found that precursor pressures needed to generate secondary reactions are typically more than 10 times the pressures of the experiments reported here; thus, this type of emission has very limited appearance in the spectra. The most apparent secondary product feature found in all five precursor spectra is the 1600 cm^{-1} C═C stretch of vibrationally excited 1,3-butadiene, which appears most likely through secondary reactions of vinyl with the parent molecules (rather than vinyl−vinyl recombination due to the low vinyl concentration). At even higher pressures, ∼100 times the pressures of the experiments shown here, there is collision-induced vibrational energy transfer between the excited photoproducts and the parent molecule generating its own molecular IR emission signature of the precursor molecule.

The remaining features common to all five precursors are attributed to the vinyl radical. There are a large number of weak transitions which appear below 2000 cm^{-1}. Assignment can be

TABLE 1: Frequencies (in cm^{-1} with uncertainty) and Intensities (in [ ] brackets relative to the strongest, which is set as 100) of the Fundamental Transitions of the Vibrational Modes of Vinyl-h_3 and Vinyl-d_3[a]

	vinyl-h_3					vinyl-d_3		
			other experimental work					
normal modes	previous report[b]	this work	in gas	in matrix	calc. results[k]	this work	other matrix results	calc. results[l]
ν_1 (a′) α-CH stretch	3235 ± 12/[7]			3141[f]	3298/[1.4]		2348[f]	2480
ν_2 (a′) CH_2 a-stretch	3164 ± 20/[11]			2953.6[f]	3222/[6.1]		2192.5[f]	2387
ν_3 (a′) CH_2 s-stretch	3103 ± 11/[0.5]		2901[c]	2911.5[f]	3118/[6.0]		2124.1[f]	2259
ν_4 (a′) CC stretch	1700 ± 35/[0.1]	1595 ± 10/[3.3]			1689/[1.4]			1593
ν_5 (a′) CH_2 s-bend	1277 ± 20/[100]	1401 ± 5/[4.2]		1357.4,[f] 1356.7,[g] 1353.2,[h] 1248.9[i]	1419/[10.6]	1060 ± 15/[7.2]	1000.4,[f] 996.5,[h] 993.8[i]	1028
ν_6 (a′) CH_2 a-bend + α-CH bend	1099 ± 16/[43]	1074 ± 8/[6.9]			1077/[12.5]	820 ± 6/[9.4]		835
ν_7 (a′) CH_2 + α-CH a-bend	758 ± 5/[93]		674[d]	677.1[f]	730/[29.8]			570
ν_8 (a″) CH_2 + α-CH s-oop bend	955 ± 7/[32]	944 ± 6/[100]		895.3[f]	965/[100]	728 ± 9/[100]	704.8,[f] 704,[j] 701.7,[h] 698.9[i]	760
ν_9 (a″) CH_2 + α-CH a-oop bend	895 ± 9/[11]	897 ± 6/[65]	895[e]	857,[f] 900.8,[g] 896.6,[h] 891,[i] 900[j]	850/[13.7]		654.5[f]	659

[a] Previous work, this work, other gas and matrix phase results, as well as calculations are included for vinyl-h_3. Results from this work and matrix results are presented for vinyl-d_3. The calculated results for vinyl-d_3 are generated by utilizing the theoretical frequencies from ref 54 and a DFT calculation to provide the isotopic frequency ratio. [b] Data from ref 1. [c] Data from ref 81. [d] Data from ref 13. [e] Data from ref 33. [f] Vinyl in Ne data from ref 41. [g] Vinyl in Ar data from ref 37. [h] Vinyl in Kr data from ref 37. [i] Vinyl in Xe data from ref 37. [j] Vinyl in Ar data from ref 36. [k] Data from ref 54. [l] Calculated using results from ref 54 and DFT isotopic ratios.

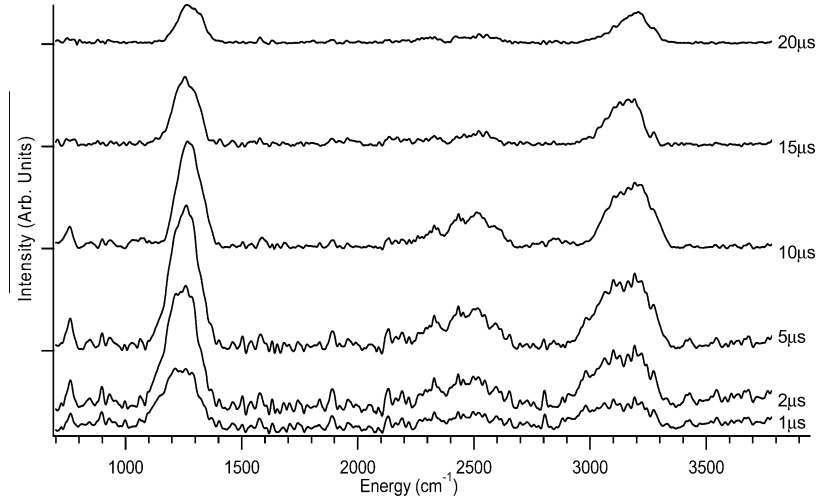

Figure 2. Selected time slices, 1, 2, 5, 10, 15, and 20 μs, of IR emission spectra following photodissociation of vinyl bromide. No acetylene filter was used.

made based on emission frequency overlap between the different precursor photolysis experiments. Common features exist at ~775, 900, 950, 1050, 1400, and 1600 cm^{-1}. The assignment of these features can be further ascertained utilizing the 2DCSC analysis method discussed below.

B. IR Emission Spectra Containing Features from Vinyl-d_3. The reaction energetics and dissociation pathways of the deuterated precursor species should be similar to the nondeuterated ones. The emission spectra recorded, without the acetylene gas filter, for the photolysis of VBr-d_3, VCl-d_3, and 13BD-d_6 are shown in Figure 3. These time-resolved IR emission spectra are dominated by two common features at 1000 and 2300 cm^{-1}. As in the nondeuterated systems, the only common reaction product other than vinyl that appears to emit in the IR is acetylene-d_2 with its $\nu_4 + \nu_5$ combination band at 1042 cm^{-1} and the ν_3 CD stretch at 2439 cm^{-1}. At longer detection times, typically 10 μs and longer, rotational structure can be seen in both emission features.

Partially resolved rotational lines are observed for DBr and DCl between 1500 and 2100 cm^{-1} for the photolysis of VBr-d_3 and VCl-d_3, respectively. Intensities for the DBr and DCl bands are less than those seen for HBr and HCl, as expected due to the increase in mass. No other strong emission features are observed.

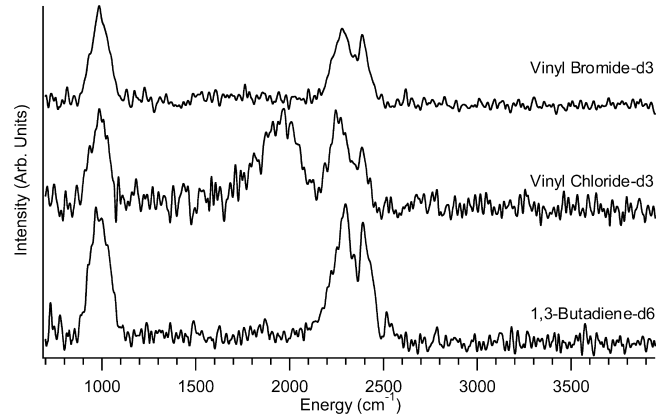

Figure 3. IR emission spectra recorded in between 2 and 3 μs following the photolysis of vinyl bromide-d_3, vinyl chloride-d_3, and 1,3-butadiene-d_6. No acetylene-d_2 filter was used.

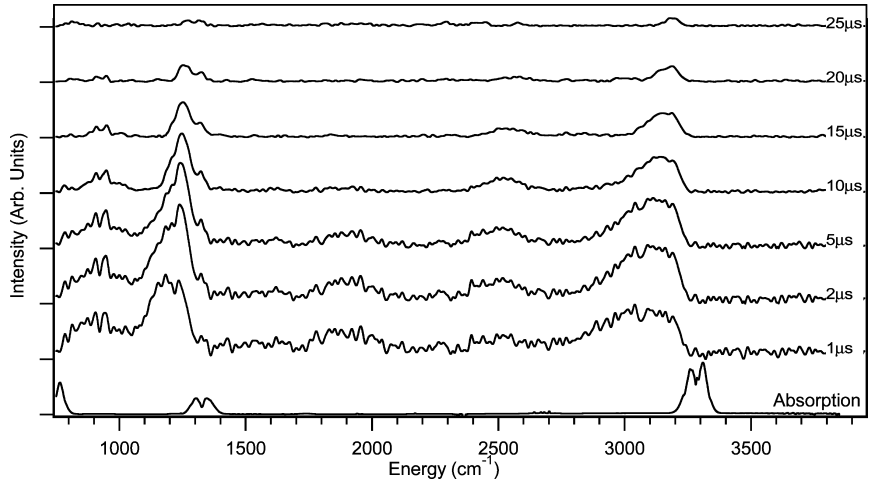

Figure 4. IR emission spectra, obtained with the acetylene IR filter for times following the photolysis of vinyl bromide. Seven time slices are shown corresponding to 1, 2, 5, 10, 15, 20, and 25 μs following photolysis. The absorption spectrum of room-temperature acetylene is shown in the lower graph. The emission curves are normalized to the total emission signal. The absorption spectrum is normalized independently.

The temporal behavior of the isotopically substituted molecules behaves analogously to the nondeuterated molecules. Longer peaking times and decay constants are observed for the acetylene-d_2 emission when compared with the vinyl-d_3 bands. There is again an extra feature in the 1000 cm^{-1} band in the 13BD-d_6 spectra that peaks and decays faster than the rest of the intensity, which can thus be attributed to arising from another emitter. This emission shares a similar fast time decay when compared to the same vibrational modes, accounting for isotopic shift, in the nonisotopically substituted 1,3-butadiene.

The remaining features, three weak bands at ~725, 825, and 1050 cm^{-1}, which are common to all three spectra, seen in Figure 3, can be attributed to vinyl-d_3. There are fewer emission bands present in the isotopically substituted spectra than in the vinyl-h_3 case because some of the bands which involve deuterium atoms shift to lower frequency and out of the detection range. Once again, 2DCSC described below will aid in determining the exact frequency more accurately.

C. The Effect of Filtering IR Emission by Room-Temperature Acetylene. The room-temperature acetylene cell placed in between the photolysis region and the FTIR should filter out the emission in resonance from the absorption transitions of room-temperature acetylene. The filtered out transitions include the fundamental transition of ν_3 and ν_5 as well as the $\nu_4 + \nu_5$ combination band in all of the spectra.

The filtering of the IR emission is achievable within the bandwidth of the fundamental rovibrational lines. There are two main contributions to the bandwidth. At the low filter pressures of ~10 Torr, collisional broadening contributes approximately 0.003 cm^{-1}. At higher pressures up to 100 Torr, used in some of the filtering experiments with strong IR emission from the photolysis, the pressure broadening becomes comparable to the Doppler width of 0.007 cm^{-1}. Higher vibrational transitions that do not overlap with the fundamental transitions are not filtered by the room-temperature cell. Rotational bands generated by acetylene molecules with a high rotational temperature will also pass through the cell unaltered.

The IR filtering result is shown in Figure 4. The series of spectra shown here represent several time slices, 1, 2, 5, 10, 15, 20, and 25 μs following the photolysis pulse. Also shown is the cold acetylene absorption spectrum at the bottom. Absorption and emission spectra are scaled independently. The effect of the acetylene gas filter is clear for the ν_5 mode at 730 cm^{-1}, the $\nu_4 + \nu_5$ mode at 1328 cm^{-1}, and the ν_3 mode at 3289 cm^{-1}. At later time, the two main features (ν_3 and $\nu_4 + \nu_5$) in the emission spectra are almost completely filtered out. The effect of acetylene absorption of emission is also clear when the filtered spectra in Figure 4 are compared to the unfiltered spectra in Figure 2. At early time, the filter removes emission intensity from the blue side of the anharmonically shifted $\nu_4 + \nu_5$ and ν_3 modes. Artificial peaks are generated at 1325 and 3300 cm^{-1}, which lie between the rotational bands of the $\nu_4 + \nu_5$ and ν_3 modes, respectively. This is due to the acetylene gas filter acting as a band-pass filter and selectively filtering the emission signal within the room-temperature rotational band.

IV. 2D Cross-Spectral Correlation Analysis

The emission bands assigned to vinyl-h_3 and vinyl-d_3 are weak and fast decaying, thus making definitive assignments difficult, even with the aid of multiple precursors. They can, in principle, be identified to arise from a common source through a correlation analysis. A common transient source of emission will show similar temporal behavior in intensity and frequency even when generated through different reaction pathways or from different precursors entirely. These emission features from a common source, displaying similar time dependence, can be expressed with similar phase functions in a Fourier analysis. A correlation analysis can then be employed to identify these phase-matched features and enhance the S/N ratio in the spectra.

The 2DCSC analysis was developed,[56] based on the general two-dimensional correlation analysis, for deciphering correlations among spectral features from two different spectra. Briefly, the time-dependent intensity at each frequency in each spectrum is subjected to Fourier analysis and represented by a set of phase-coded sinusoidal functions. The phase correlation among the two spectra generates a pair of two-dimensional maps, the synchronous and asynchronous maps. The synchronous map is generated by the positive overlap of the phase information for common features. The diagonal of the synchronous correlation map can be extracted to display an enhanced *S/N* ratio for the correlated features in the spectra. The asynchronous map represents features with different phase information anticorrelated on the off-diagonal points. Features from a common source will show a correlated behavior on these off-diagonal points.

The cross correlation takes advantage of different precursor molecules producing the same radical of interest. Uncorrelated features including random and nonrandom noise are subse-

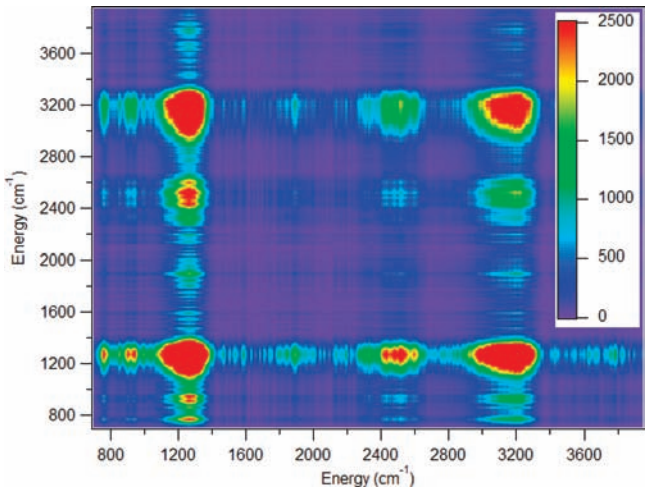

Figure 5. 2DCSC synchronous map for the VBr−13BD correlation pair. The color scheme for the relative magnitude is shown on the right.

quently reduced. A 5−10 times enhancement of the *S/N* ratio has been found by utilizing the 2DCSC analysis.[56,67] The correlation diagonals from different possible pairs are extracted from their synchronous maps to display the common emission features with enhanced *S/N*; the correlated spectral peaks appear with enhanced intensity, while the noise as uncorrelated intensity is suppressed. We can further enhance the *S/N* by combining the different correlation diagonals from different pairs of precursors, producing a spectra that is representative of common emission features from five different sources.

A. Analysis of Spectra Containing Vinyl-h_3 Emission. The main source of spectral information is found in the synchronous map generated from the 2DCSC analysis. A sample map for the VBr and 13BD unfiltered emission experiments is shown in Figure 5. Strong correlations involving the two main features at 1100−1400 and 3000−3300 cm^{-1}, corresponding to emission from the $\nu_4 + \nu_5$ and ν_3 modes of acetylene, respectively, are evident. In addition, there are less intense correlation features near 1900 and 2500 cm^{-1}. The 2500 cm^{-1} feature may arise from HBr emission and possibly weak overtones of acetylene, $2\nu_4 + 2\nu_5$ at 2260 and $\nu_2 + \nu_5$ at 2703 cm^{-1}. The 1900 cm^{-1} emission may arise from the combination $2\nu_4 + \nu_5$ acetylene mode at 1941 cm^{-1}. The two main emission features at 1100−1400 and 3000−3300 cm^{-1} are so strong that they generate off-diagonal correlation features with all other observed emission. In the low-frequency bending region from 700 to 1700 cm^{-1}, there are off-diagonal components at 765, 855, 895, 945, 1000, 1040, 1065, 1410, 1475, 1540, and 1590 cm^{-1}, in addition to the main feature that stretches from 1100 to 1400 cm^{-1}. Only some of these features correspond to vinyl emission.

One way to utilize the correlation diagram to efficiently view the positive correlation between the two correlated spectra is the diagonal of the synchronous map.[56] The diagonal displays the peaks that commonly exist in both spectra, and its magnitude corresponds to the strength of the correlation. The vinyl radical's 5 precursor molecules allow a total of 10 independent 2DCSC diagonals to be generated. All 10 synchronous diagonal spectra are shown in Figure 6. The correlation diagonals are generated from unfiltered emission spectra. The correlation diagonals are obtained using all (∼500) of the observable emission spectra in the typical time span from 0 to 50 μs. Emission features with varying intensity are identified in five distinct regions in the correlations, as labeled in the figure. In region 1, there is some low-intensity bending mode emission that is detectable down to the detector cutoff at ∼700 cm^{-1}. The most prominent peak at around 1275 cm^{-1} in the spectra occurs in region 2 with several weak, close-lying but visibly independent emission bands to the red and blue of this main feature. These other bands show a faster decay rate when compared with the main feature. There are some small features that lie just to the blue of region 2, one of which is common to all of the spectra but most just being noise. Region 3 contains a feature that can be attributed to the very intense CO stretching mode at 2145 cm^{-1} produced in the photodissociation of methyl vinyl ketone. Even though the other precursors do not produce CO, the intensity of the CO emission in the MVK spectra, being several orders of magnitude higher than any other emission in all precursor spectra, spills over into the correlation diagonal.

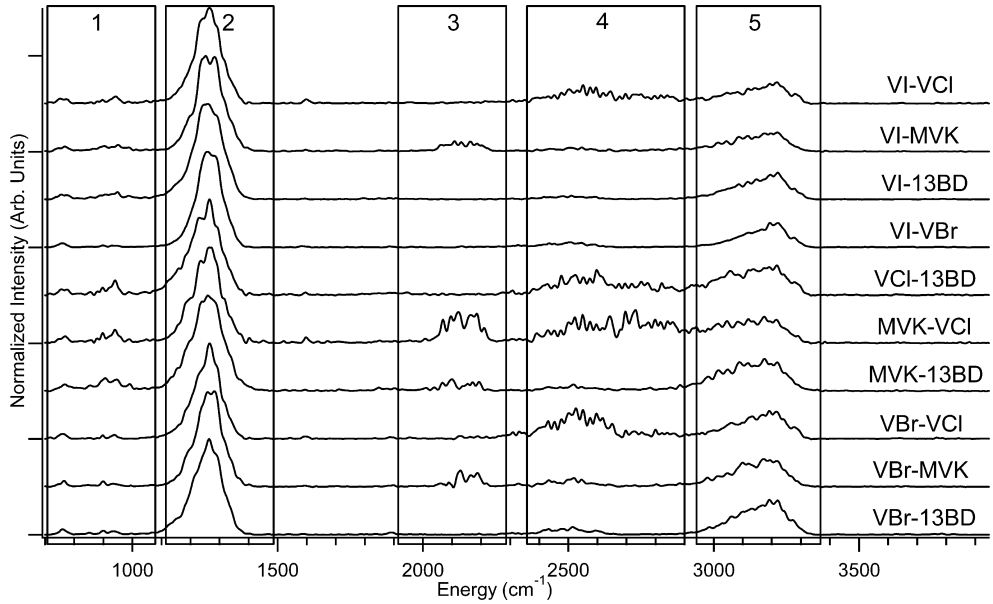

Figure 6. 2DCSC synchronous diagonals of the 10 correlation pairs from the 5 precursors. The spectra are grouped into five regions, labeled 1−5, for discussion. Each curve is normalized independently and shown on the same scale. The correlation diagonals are generated from unfiltered spectra. The complete emission signal, typically from 0 to 50 μs, is included in the correlations.

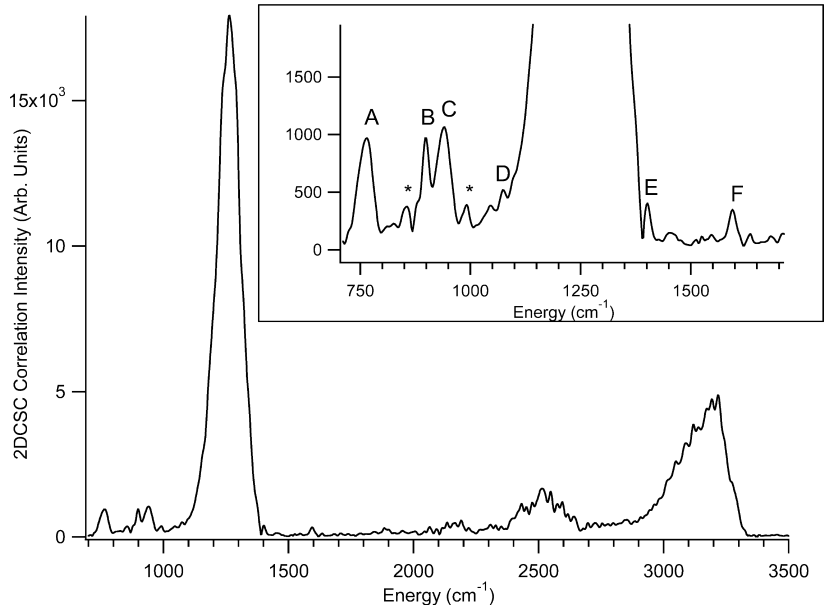

Figure 7. The geometric mean (GM) correlation of the square root of each of the 2DCSC diagonals in Figure 5 in the region from 700 to 3500 cm^{-1}. The inset curve represents 10 times magnification in the region of 700−1700 cm^{-1}. Labeled peaks (A−F) are discussed in the text. The * represent rotational bands of the two oop bending modes of vinyl. The curve is generated from the correlation diagonals of unfiltered correlation spectra from Figure 6.

This feature does not appear in the correlations without MVK. Region 4 contains HBr and HCl emission, located between 2300 and 3100 cm^{-1}, generated from VBr and VCl photolysis. There is also an unresolvable feature in the spectra from VI, MVK, and 13BD where no HBr or HCl is generated. This weak feature has no discernible structure nor any detectable anharmonic shift. Though this feature lies close to the $\Delta v = 2$ transition for the combination $2\nu_4 + 2\nu_5$ mode of acetylene and the strength of the combination band suggests that this overtone band, though weak, can be observed, the true origin of this feature remains undetermined. All CH stretching is observed in region 5 as an unresolved feature. The ν_3 CH stretch of acetylene at 3289 cm^{-1} appears at the blue side of the region. The large irresolvable emission observed in region 5 prohibits further analysis even with the aid of the 2DCSC technique. We expect the three stretching modes of vinyl to be much weaker compared to the bending modes assigned below.[54] This feature can be assigned to the ν_3 emission from acetylene based on modeling of the rotational contour, anharmonic shift, and intensity.[57] There may be a small amount of emission on the red end of the feature assignable to vinyl. A lack of corresponding features found in the deuterated results as well as the weak nature of these features, however, prohibits a definitive assignment here.

Each of the 10 diagonals obtained from 2DCSC represents a correlated spectrum between the two sets of time-resolved emission spectra. Comparing the correlation pairs shown in Figure 6, one notices that not all pairs have the same intensity ratios between the spectral peaks. For example, the relative intensity of the two vinyl emission features at 897 and 944 cm^{-1} varies between the different correlation pairs. This is due to several reasons. Vinyl radicals are generated with different amounts of internal energy depending on the precursor used. Thus, vinyl emission may exhibit slightly different temporal decay/frequency shift characteristics. In addition, there are other factors influencing the correlation intensity, including emission from other sources, systematic and random noise, and pressure fluctuations (~5%) during the experiments. Because of these experimental artifacts on the correlations, the correlation diagonals are used only for frequency determination. The correlation spectra are particularly useful for vinyl as the vinyl radical is produced with low amounts of internal energy and the vinyl peaks are not expected to display much shift with time[45] (see the discussion on the energetics of the photolysis reactions below). Spectral intensities reported are determined directly from the experimentally observed spectra.

The product of all correlation diagonals provides a presentation of the common spectral features in all correlated spectra with much enhanced *S/N* for identifying where the spectral peaks are located. The magnitude of the points along the diagonal of each pair of spectra is numerically proportional to the product of the spectral intensities. The apparent intensity ratios of the features in the product of the 10 diagonals are approximately proportional to the 20th power of the original values.[56] The features that appear in all of the spectra are greatly enhanced in magnitude, whereas the noise, uncommon to all spectra, is dramatically suppressed. While the "intensity" in the product spectra is greatly altered from the actual strength, the spectral frequency remains accurate throughout the analysis for peaks that show little anharmonic shift with time.[67] The overall correlation of all emission spectra can be approximately represented by the 20th root of the product of the 10 diagonals. The resulting spectrum is referred to as the geometric mean (GM) correlation, with its magnitude directly in proportion to the relative spectral intensity. The GM correlation is shown in Figure 7.

The result shown here is from the correlation diagonals of unfiltered emission spectra. The two main features, 1100−1400 and 2900−3300 cm^{-1}, correspond to hot bands of the $\nu_4 + \nu_5$ and ν_3 modes of acetylene. There are several features in the low-energy region which will be discussed shortly. There is also some intensity between 2000 and 2700 cm^{-1}, which may arise from other emission products HBr, HCl, and CO. There is, however, some emission from other combination bands of acetylene, namely, $\nu_2 + \nu_5$ at 2703 cm^{-1}, $2\nu_4 + 2\nu_5$ near 2660 cm^{-1}, $3\nu_5$ at 2170 cm^{-1}, and $2\nu_4 + \nu_5$ at 1941 cm^{-1}. Assignments of these bands are difficult due to their low intensity and overlap with other emission features.

TABLE 2: Major Products and Exothermicities of 193 nm Photolysis of the Five Precursor Molecules[a]

precursor molecule	photolysis product	ΔH (kcal/mol)
C_2H_3Cl	$C_2H_3 + Cl$	−58
	$C_2H_2 + HCl$	−123.7
C_2H_3Br	$C_2H_3 + Br/Br^*$	−69/−59
	$C_2H_2 + HBr$	−123
C_2H_3I	$C_2H_3 + I/I^*$	−86/−79
	$C_2H_2 + HI$	−122
$CH_3COC_2H_3$	$CH_3 + C_2H_3 + CO$	−46.4
	$CH_3 + C_2H_2 + H + CO$	−9.1
C_4H_6	$C_2H_3 + C_2H_3$	−31
	$C_2H_4 + C_2H_2$	−108

[a] Only those channels generating vibrationally excited products that are detectable through IR emission are listed. VCl, VBr, and VI enthalpies are taken from ref 79, while MVK and 13BD are from ref 1. The * indicates electronic excitation.

The inset in Figure 7 represents a 10× magnification of the GM correlation spectrum at 700−1700 cm^{-1}, which shows several features in the low-energy bending region. Feature A coincides with the unfiltered portion of the R-branch of the ν_5 mode of acetylene, though it decays faster than other acetylene peaks. The remainder of this emission feature is cut off due to the falloff of the detector. Features B and C are assigned to the out-of plane-modes, ν_9 and ν_8, respectively, of the vinyl radical. Agreement with theoretical calculations and rotational band contour fitting, discussed below, support this assignment. Peaks D and E are assigned to vinyl even though they are in close proximity to the most intense acetylene feature. These features cannot be from acetylene; peak D lies too far to the red to be from highly vibrationally excited acetylene, while peak E lies over 70 cm^{-1} to the blue of the acetylene $\nu_4 + \nu_5$ band. Peak F can be assigned to the C═C stretch of vinyl. Its fast time decay profile matches the other features attributed to vinyl. This feature should not arise from the secondary reaction product 13BD because the low precursor pressure used in our experiment greatly reduces secondary reactions. In addition, emission from 13BD has only been observed in higher-pressure experiments and at a much later time.[1,62]

The band centers of the assigned features correlate well with those harmonic frequencies reported by Sattelmeyer and Schaefer.[54] The accuracy of the harmonic frequencies generated by EOMIP-CCSD/cc-pVQZ has been stated to be within 100 cm^{-1} of experimental frequencies without anharmonic corrections.[68,69] However, linear correlations between experimental anharmonic results and harmonic calculations have yielded corrections of ∼0.95−0.96[55,70−72] depending on the molecule and level of theory used. Nonetheless, we expect the frequency correction to be small because of the low frequencies of modes in the bending region. In addition, the low-frequency vibrations do not exhibit a detectable shift in frequency as seen in Figure 2, even with 30−80 kcal/mol (see Table 2) of internal energy.

All assigned low-energy vibrational modes are listed in Table 1 together with the calculated vibrational frequencies for comparison. All reported experimental frequencies were obtained from band contour fitting. Rotational fits were used for ν_8 and ν_9, while Gaussian profiles were used for the remaining features.

During the entire data collection time period following the photolysis of the precursor molecule, many species emit IR signal with different time behavior. These species include primary photolysis and secondary reaction products. In the overall 2DCSC, correlations appear for all pairs of emission features and render the diagram complex for interpretation. This complexity may be reduced if the time period for correlation examination is restricted to a shorter duration. For example, if the correlation is restricted to the initial time period, the emission features from the primary reaction products are dominant while the contributions from the secondary products are reduced. This practice of correlation with reduced time duration is hereafter termed "pseudotime correlation".

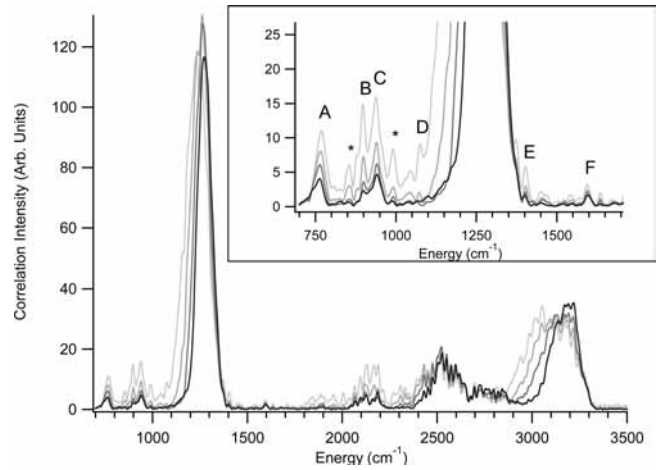

Figure 8. The GM pseudotime correlations of the 10 diagonal psedotime correlation pairs during the first 8 μs after the precursor photolysis from 700 to 3500 cm^{-1}. Each time correlation encompasses a 2 μs duration. The four correlation spectra are presented with lighter to darker shades as time progresses. The labeled peaks are the same ones as identified in Figure 7 and discussed in the text. The * represent rotational side bands for the two oop vibrations of the vinyl radical. The correlations are generated from unfiltered emission spectra. The inset is a 5× magnification of the 700−1700 cm^{-1} region.

Figure 8 shows four GM pseudotime correlations taken 2 μs apart with 20 time slices included in each correlation. The first four pseudotime correlations, corresponding to the observation time of 0−8 μs, are shown. The pseudotime correlations are taken from unfiltered spectral data. The labeling of the peaks is the same as that in Figure 7. The five vinyl features, peaks B−F, reach maximum intensity at 1−2 μs and decrease with little vibrational shift, indicating low vibrational energy content after photolysis. This is in marked contrast to the acetylene features which show much larger anharmonic shift in the ν_3 CH stretch at 3000−3300 cm^{-1} and the $\nu_4 + \nu_5$ combination band at 1100−1400 cm^{-1}. In addition, the lifetimes of the acetylene features are significantly longer than those of the vinyl features. Emission near the fundamental transitions of acetylene has been measured to be longer than the diffusion-limited 60 μs.

Because of the reduced number of time slices included in the pseudotime correlation, the spectra may contain unintended effects such as an increase in noise, as seen in the congested low-frequency region in Figure 8, and less accurate intensity representation for the spectral peaks. As the time evolution of the system is truncated and the integration windows are smaller in the pseudotime correlations, the relative spectral intensity may appear different in different sets of correlations using different time windows. This is observed in the pseudotime correlation in Figure 8, where peaks C, B, D, E, and F, which are all assigned to vinyl, appear with decreasing intensity, C > B > D > E > F. The overall correlation in Figure 7, however, shows that the intensities of peaks B and C are approximately equal, and the intensities of peaks D, E, and F are weaker with the trend D > E > F. Because of these discrepancies, the intensities are determined directly from experimentally measured, unprocessed spectra.

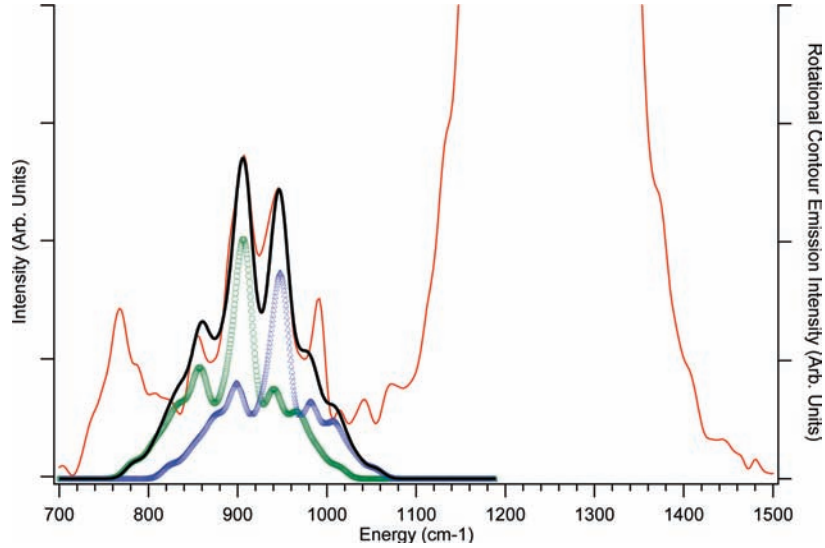

Figure 9. Band contour fitting (in black) of the features in the 800−1000 cm^{-1} region. The rotational fitting of the MVK−13BD pair is shown. The two out-of-plane vibrations (ν_8, triangle points; ν_9, circle points) of the vinyl radical contribute to the emission features. The MVK−13BD correlation pair is generated from unfiltered emission spectra.

One of the two out-of-plane bending modes has been previously determined at 897 cm^{-1} by high-resolution techniques.[33−35] Recent ab initio calculations have placed the two out-of-plane modes at 850 and 965 cm^{-1}.[49,54,73,74] The rotational band contour of the two C-type transitions is modeled here using an asymmetric rotor calculation (XASYROT)[75] with rotational constants either measured by Kanamori[33] or calculated by Gaussian 03.[76,77] The rotational band contour fits were performed on the 2DCSC diagonal spectra. One such correlation diagonal spectrum and its rotational contour fit for both the 897 and 944 cm^{-1} bands are shown in Figure 9. The rotational contour fitting of the correlation diagonal of MVK and 13BD is shown. The correlation diagonal is generated from unfiltered emission spectra. Note that in fitting the 2DCSC diagonal spectrum, the intensity of the rovibrational transitions is squared. In the rotational band contour calculation, a Watson asymmetric top Hamiltonian with A-reduction[75,78] was used to generate rotational states for the lower and upper vibrational levels independently. Molecular constants, transition types, and nuclear spin statistics for the vinyl modes have been previously established.[33] To diagonalize the Hamiltonian matrix for the near-prolate symmetric rotor (A > B ∼ C), representation I^r was utilized to define the inertial axes. The emission transitions are from a rotational population defined by a temperature. Only first-order transitions with $\Delta K = 0, \pm 1$ are included. A least-squares fit was performed to yield two band centers at 897 and 944 cm^{-1} with a rotational temperature of 350 K. This temperature is justifiable. Vinyl molecules may be generated with a high degree of rotational energy; however, several hundred collisions with the buffer gas would have cooled the rotational temperature. The bandwidth resolution of 12 cm^{-1} was imposed in the calculation. It is found that the temperature is weakly correlated with the resolution width.

B. Analysis of Spectra Containing Vinyl-d_3 Emission. Isotopic substitution of the three vinyl radical precursors, VBr-d_3, VCl-d_3, and 13BD-d_6, has the distinct advantage of producing deuterated vinyl, C_2D_3, which affords the opportunity to test the C_2H_3 assignments through the isotope effect. It is anticipated that the frequency of the vibrational mode will change according to the change of the normal mode mass while the intensity remains relatively unchanged with respect to the unsubstituted molecule. Through complete deuteration of the molecules, each vibrational mode containing H/D motion in the vinyl molecule will display a vibrational frequency shift of ∼1.3 from the deuterated to the hydrogenated molecule, Table 1. The only exception to this is the ν_4 C═C stretch, whose mass contains very limited contribution from the H/D atoms and thus shows a very small isotopic shift of 1.06. The isotopic ratios of the vibrational frequencies in Table 1 were calculated through Gaussian 03[76,77] DFT calculations utilizing the 6-311+G(d,p) basis set.

Spectra taken from deuterated precursor photolysis show emission from vinyl-d_3 as well as acetylene-d_2. Figure 10 displays the GM correlation spectrum of the three correlation diagonals obtained from the three precursors. The result is based on the unfiltered deuterated emission spectra. The lower quality of the deuterated GM correlation is due to the decrease in the number of possible correlation pairs as compared to the nondeuterated result. Only three bending modes of vinyl-d_3 could be identified primarily because of the detector cutoff at ∼700 cm^{-1}. Features C, at 728 cm^{-1}, with some rotational structure displayed on the blue side, and D, at 820 cm^{-1}, are clearly visible and correlate well with the corresponding vinyl-h_3 peaks in both frequency and intensity. Feature C has a H/D ratio of 1.30 compared to the calculated value of 1.27. Feature D has a ratio of 1.31 compared to 1.29 determined from the calculation. The combination band of acetylene once again dominates the low-energy region; however, there is another feature, E, that appears as a shoulder on the strong acetylene band. Feature E is assigned to the ν_5 bending mode of the vinyl-d_3 radical based on pseudotime correlation analysis, presented in Figure 11, which allows this shoulder to be separated from the main peak. Feature E displays a 1.32 H/D frequency ratio compared with the calculated value of 1.38. This slightly larger difference between the experimental and theoretical values may have been caused by the uncertainty in the determination of the band centers because of the close proximity to the strong acetylene band. The only other feature in the deuterated correlation diagonal is the CD stretch of acetylene-d_2 between 2000 and 2400 cm^{-1}.

The GM pseudotime correlation spectra of the deuterated molecules are shown in Figure 11 in the range of 700−3500 cm^{-1}. The inset is a 2.5× magnification of the 700−1550 cm^{-1} region. These correlations are generated from unfiltered deu-

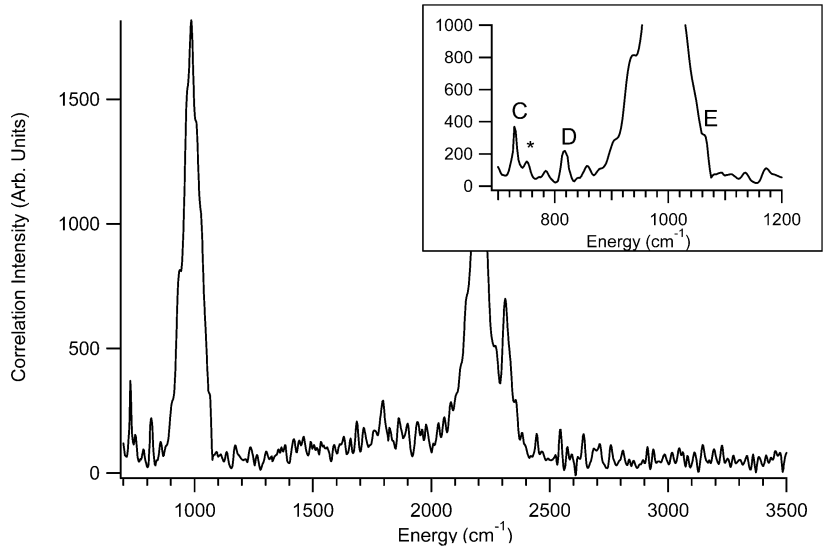

Figure 10. The GM of the set of 2DCSC diagonals of the correlation pairs from the three deuterated precursors in the region of 700−3500 cm^{-1}. The inset represents a 1.5× magnification of the 700−1200 cm^{-1} region. The labeled peaks have the same assignment as the vinyl-h_3 radical seen in Figure 7. Some rotational bands appear near peak C, which are labeled with an *. The deuterated result shown here contains correlations of unfiltered emission spectra.

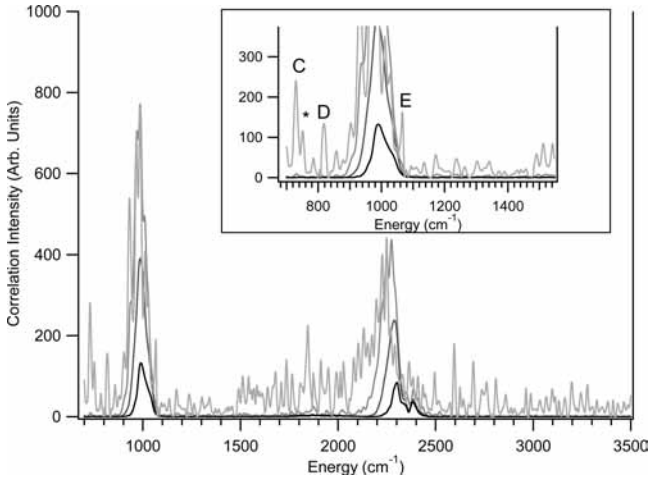

Figure 11. Three GM pseudotime correlations, each of 2 μs duration, for the first 8 μs after the photolysis of the deuterated precursors in the range of 700−3500 cm^{-1}. The inset is a 2.5× magnification of the 700−1550 cm^{-1} region. They are presented with lighter to darker shades as time progresses. Labeled peaks share the same assignment as in Figure 7. Some rotational bands appear near peak C and are labeled with an *. The correlations are generated from unfiltered emission spectra.

terated emission spectra. Four GM pseudotime correlations are shown. Each correlation contains 2 μs of emission spectra (20 spectra). The acetylene-d_2 $\nu_4 + \nu_5$ combination and ν_3 CD stretching bands at 985 and 2100−2400 cm^{-1} show significant anharmonic shifts, while the vinyl-d_3 bands, as expected, do not, confirming the vinyl assignment. The three vinyl bands assigned in Figure 10, peaks C, D, and E, are observed in the pseudotime correlations in Figure 11. The deuterated precursor pseudotime correlation seen in Figure 11 can also be compared with the pseudotime correlation for vinyl-h_3 shown in Figure 8. Assignments for features C and D in Figure 10 are analogous to assignments made from Figure 8. In comparison with the overall correlation spectrum, feature E in the earliest time pseudocorrelation appears as an isolated peak, as opposed to a shoulder in Figure 10. Features C, D, and E decay immediately, with time constants of $\tau \sim 0.5$ μs^{-1}, which are similar to the time constants recorded for vinyl-h_3 features. In contrast, acetylene-d_2 displays a later peak time, has a longer decay time, and shows more anharmonic shift in frequency.

V. Discussion

A. Precursor Photolysis. The main products of vinyl halides following 193 nm photolysis include vinyl + halogen radicals from the atomic channel and acetylene + hydrogen halide from the molecular channel. The atomic/molecular elimination channel ratio increases with the halide atom size (0.48, 0.56, >0.8 for VCl, VBr, and VI).[79] This trend can be understood from a combination of their respective carbon−halogen bond energies (95.0, 78.8, and 61.9 kcal/mol) and the relatively unchanged molecular elimination channel heats of reactions (27.1, 26.6, and 25.9 kcal/mol for VCl, VBr, and VI, respectively).[17,79] Subsequently, it is understandable that there is a lack of emission from HI after photolysis of VI while there is a significant amount of HCl and HBr emission from their respective precursors.

Molecular elimination channels producing HCl and HBr with acetylene from vinyl bromide and vinyl chloride have been extensively studied.[19,62,63] HCl emission up to $v = 7$ and HBr emission up to $v = 6$ have been recorded as early as 1 μs after the 193 nm photolysis pulse. The HCl/C_2H_2 emission channel has been determined to have a bimodal rotational distribution for HCl of 500 and 9500 K. The branching ratio between the two matches the ratio of the reaction channels of 0.81:0.19 for three-center, high-J to four-center, low-J rotational distribution. Vinylidene is generated with an internal energy of 35 kcal/mol, and its isomerization to acetylene produces a nascent energy of 76 kcal/mol.[80] The HBr/C_2H_2 emission channel has been determined to primarily arise from a three-center elimination yielding HBr with vibrational and rotational temperatures of 8690 and 7000 K, respectively, and vinylidene with 24 kcal/mol of internal energy.[63] Fast isomerization from vinylidene to acetylene leaves 64 kcal/mol of internal energy in the stable product.

The lack of HI emission after the photolysis of VI is due to the lower yield of the molecular elimination channel. However, vibrationally hot acetylene is still observed. We attribute the vibrationally excited acetylene to the secondary dissociation of vibrationally excited vinyl. As has been previously determined,[13]

the energy required to dissociate the vinyl radical into acetylene is 33 kcal/mol, leaving up to 53 kcal/mol available, after the sequential bond breaking of VI, for acetylene and atomic hydrogen and iodine.

The atomic elimination channel produces vinyl + halogen radicals with 53.5, 69.7, and 86.6 kcal/mol of energy following photolysis of VCl, VBr, and VI, respectively. Those photolysis exothermicities are significantly less than their corresponding molecular elimination channels (121.4, 121.9, and 122.6 kcal/mol for VCl, VBr, and VI).[79] This offers a possible thermodynamic explanation for why the emission signal obtained from vinyl is not significantly anharmonically shifted as opposed to what is observed with the features from highly vibrationally excited acetylene.

The photodissociation of 13BD is dominated by emission from acetylene. No emission from vibrationally hot ethylene, the reaction coproduct, however, is detected. The acetylene emission shows a strong anharmonic shift at early time, indicating acetylene production with a large amount of vibrational energy. The vinyl peaks, however, do not show a strong red shift, indicating production with little vibrational excitation. This observation is consistent with exothemicity values of −31 and −108 kcal/mol for vinyl and acetylene dissociation pathways, respectively.

Sequential dissociation of methyl vinyl ketone allows for a sufficient amount of internal energy to be partitioned into the vibrational modes of vinyl; however, production of vibrationally hot acetylene has not been detected prior to this work. On the basis of the dissociation of acetone, the methyl radical exits the reaction with 8.4 kcal/mol of internal energy, leaving 37.8 kcal/mol of internal energy in the vinyl and CO coproducts. Vinyl radicals therefore have a small amount of internal energy available and thus do not exhibit a large shift in frequency observed for highly energetic molecules such as acetylene. Vinyl dissociation to ground-state acetylene requires 33 kcal/mol. It is therefore unlikely that there is any acetylene emission produced from this channel. Another mechanism must exist for the production of hot acetylene. One possibility for the production of the acetylene emission features observed in the photolysis of MVK is a concerted three-center elimination, with the products being vinylidene and acetaldehyde. This concerted channel involving two bond breakings and two bond formings should be more exothermic, leaving a larger amount of energy in the acetylene molecule.

B. Comparison with Noble Gas Matrix Studies. A recent absorption study on vinyl radicals trapped in solid Ne matrixes at 4 K has reported seven of the nine vibrational modes of vinyl.[41] The symmetric CH_2 stretching mode, reported as 2911 cm^{-1} in solid Ne, is close to the 2901 cm^{-1} value reported by a recent high-resolution gas-phase study,[55] though they are both substantially lower in energy than the highest-level theoretical calculation predictions of 3042[41] or 3118 cm^{-1}.[54] This comparison indicates that the matrix has limited influence on the frequency of the vibrational motion, particularly the ones with a smaller amplitude of motion. The large blue shift of the theoretical calculation could be due to a significant anharmonic correction needed for the typically anharmonic CH stretching motions.

In comparing the vibrational modes identified here with the matrix results, we have found generally good agreement, as shown in Table 1. The ν_5, ν_8, and ν_9 modes at 1401, 944, and 897 cm^{-1} assigned here lie 40−50 cm^{-1} higher in energy than the matrix results. This is understandable as interaction with the matrix may generate as much as 5% deviation from the nonperturbed value. The ν_4 and ν_6 modes were not detected in the matrix experiment and thus can only be compared with theoretical results in the next section.

There is one remaining low-energy mode detected in the Ne matrix study,[41] the ν_7 in-plane bend found at 677 cm^{-1}, which has also been observed at 674 cm^{-1} in the action spectra of vinyl.[13] This mode is close to the frequency of peak A in Figure 7, observed at 765 cm^{-1}, which was obtained without using the acetylene filter. However, the feature is filtered out by the acetylene cell, shown in Figure 4. This observation dictates that peak A should be assigned to an acetylene fundamental transition. The low-frequency ν_5 bending mode of acetylene has its fundamental transition centered at 730 cm^{-1}. As the fundamental transition of this mode is very close to the detector cutoff at 700 cm^{-1}, the red side of this emission feature may have been clipped. On the basis of this speculation, we assign this peak as a part of the R-rotational branch of the ν_5 transition. Our modeling suggests[57] that this acetylene mode with sufficient vibrational excitation and high rotational temperature shows strong emission to the blue of the fundamental transition, supporting the assignment. The time profile of this feature, on the other hand, appears to have a fast decay similar to those of the vinyl peaks, as seen in Figure 8. The temporal behavior, however, does not contradict assigning peak A to acetylene. It is likely that the rotational transitions in this feature are associated with higher rotational levels which can be quenched faster than the lower-energy levels and therefore have faster decays.

C. Comparison with Theoretically Calculated Normal-Mode Frequencies. Compared with recent theoretical work utilizing the EOMIP-CCSD/cc-pVQZ to generate the harmonic vibrational frequencies and intensities for the vinyl radical,[54] our assigned features agree well with calculated frequencies, as seen in Table 1. For all of the modes, except the ν_9 oop bending mode, the experimental anharmonic frequencies are red shifted (94, 18, 3, and 21 cm^{-1} for ν_4, ν_5, ν_6, and ν_8, respectively) from the calculated harmonic frequencies. These discrepancies can be explained by the need for an anharmonic correction for the calculated harmonic frequency in comparison with the fundamental transition frequency since the largest discrepancy appears in the stretch mode (ν_4). A simplistic DFT theory calculation utilizing the 6-311+G(d,p) basis set is performed to estimate the anharmonic correction for the ν_4 mode as 0.981, which corresponds to an anharmonic shift of 31 cm^{-1} and improves the match with the experimentally observed value.

The intensities determined from our study, 3.3:4.2:6.9:100 for ν_4:ν_5:ν_6:ν_8, also agree quite well with the calculated results of 1.4:10.6:12.5:100. The only mode where the intensity is significantly different is again the ν_9 mode. The calculated intensity is 13.7, while the measured intensity is 64.9.

There is some deviation between theoretical calculations and the experimentally determined frequencies for the C═C stretch, assigned at 1595 cm^{-1} but theoretically predicted to lie at 1689 cm^{-1}. This may be due to a larger anharmonic shift when compared to the bending modes. The weak mode was not observed in the deuterated experiments because the mode assigned is the weakest out of all of the observed vinyl modes and was only completely resolvable once the five precursor 2D correlations were combined. With this enhanced *S/N* ratio obtained from the correlation analysis, there were no observable features around the theoretically predicted value of 1689 cm^{-1}.

D. Comparison to Previously Assigned Vinyl Vibrational Modes. In this work, five of the nine vinyl (C_2H_3) modes are presented. The absence of assignment for the ν_7 mode is due to

the low-frequency cutoff of the detector, as well as interference from the relatively strong emission from the ν_5 mode of acetylene. With respect to the ν_1, ν_2, and ν_3 stretching modes, the irresolvable feature which contains emission from the ν_3 emission from acetylene prevents accurate determination of their positions and therefore assignment. An accurate assignment of these modes will require production of vinyl in the absence of vibrationally hot acetylene or via high-resolution studies, of which the ν_3 mode has recently been observed.[81]

For the remaining five vibrational modes, there are two primary improvements in comparison with our first report.[1] The strong 1275 cm^{-1} band that appeared in the emission spectra following the photolysis of all precursors and was assigned to the ν_5 mode has now been assigned to an unexpectedly strong combination band emission from hot acetylene. The ν_5 mode has now been identified and assigned at 1401 cm^{-1}, with the frequency and intensity consistent with theoretical calculations. In addition, the ν_4 mode has been identified and assigned at 1595 cm^{-1}. This mode is the weakest and subsequently only appears very briefly in the emission spectra following photolysis. The application of the 2DCSC technique enables the peak position to be better determined in the average correlation diagonal curves. The remaining modes ν_6, ν_8, and ν_9 along with the ν_6 and ν_8 modes from the deuterated vinyl are consistent with the previous report.

E. Vinyl-d_3 and the Isotope Effect. The deuteration of the vinyl radical precursors has allowed the detection of three vibrational modes, ν_5, ν_6, and ν_8, of vinyl-d_3. Their experimentally determined values of 1060, 820, and 728 cm^{-1} compare with the theoretical values of 1028, 834, and 759 cm^{-1}, which are calculated from the theoretical frequencies for hydrogenated vinyl and the isotopic ratios from the DFT calculation. The intensities of these transitions (7.2:9.4:100) agree well with both the theoretical (10.6:12.5:100) and experimental (4.2:6.9:100) values for the vinyl-h_3 molecule. The ν_5 and ν_8 bands of the deuterated molecule also compare well with the vinyl-d_3 in solid Ne work,[41] with the ν_5 and ν_8 modes deviating higher by 6 and 3%, respectively. The ν_6 mode was not detected in the matrix experiment, even though it was predicted to be as intense as the ν_5 mode in this work. In addition, the solid matrix absorption work observed CH (and CD) stretches that have been predicted[54] to be less intense than this unobserved mode. A possible reason for this missing feature in the matrix work could be that the ethylene precursor ν_7 mode absorbing at 950 cm^{-1} overshadows the ν_6 vinyl band.

F. Emission from Highly Vibrationally Excited Acetylene. The 2DCSC analysis and the isotope-substituted vinyl study enabled five of the six low-energy vibrational modes of vinyl to be assigned. The assignments are consistent with previous experimental measurements and theoretical calculations.[41,54] A consequence of the identification of these lower-frequency modes is that the most intense emission feature at 1300 cm^{-1} does not come from vinyl. There have been speculations on the origin of this intense peak observed in emission spectra detected from all precursors. One hypothesis proposed by Sattelmeyer and Schaeffer[54] is that this peak belongs to a vibrational motion in the electronic excited state. The width and temporal shift of this feature indicates a large anharmonicity that is consistent with an emitting species with a significant amount of rotational−vibrational energy in the emitter. This implies that the emitter is likely not electronically excited as the excitation energy is not large enough to leave substantial rotational−vibrational energy in electronically excited products.

Another possible source for this emission is the combination band of acetylene, whose band center lies at 1328 cm^{-1}.[82] Assigning this feature to a combination band would be unexpected as IR combination bands are usually much weaker than the allowed fundamental transition. The strength of the combination band intensity, on the other hand, scales approximately with the product of the vibrational quantum numbers of the two modes involved and, thus, increases sharply with vibrational energy. In the experiments where a room-temperature acetylene filter is not used, it is observed that the intensity at 1328 cm^{-1} has a much later peak time and slower decay constant, as shown in Figure 2, when compared to the vinyl bands and the emissions assignable to highly vibrationally excited acetylene. The anharmonic shift of the feature toward the fundamental transition indicates that this peak arises from the $\nu_4 + \nu_5$ combination band of acetylene. This assignment is further shown by the removal of the fundamental emission of acetylene on the blue side of the $\nu_4 + \nu_5$ and ν_3 features when the acetylene filter is used in Figure 4. We can model the IR emission at 1300 cm^{-1} as the combination band and show that it is in proportion to the CH bands at 3000−3300 cm^{-1} assigned to vibrationally hot acetylene. Details of this modeling will be reported separately.[57] This discovery has also put some restrictions on the assignments of the three CH stretching modes of the vinyl radical. The three CH stretching modes reported previously lie within the ν_3 mode of vibrationally hot acetylene. Though there is emission intensity detected to the red of this broad ν_3 emission feature that may be assignable to vinyl, the intensity is too weak and has too much interference to be accurately assigned even after the 2DCSC analysis. The stretching modes cannot be assigned in the deuterated experiment either due to the overlap of deuterated acetylene emission. This is understandable due to the fact that the frequencies of the deuterated stretching modes are shifted closer together and their intensities iares still clustered with emission from the ν_3 mode of vibrationally hot acetylene-d_2. Assignment of the CH stretching modes by this technique may only be obtained in the absence of vibrationally hot acetylene.

From prior studies of precursor photolysis, the production of abundant vibrationally hot acetylene is apparent. All precursor molecules except methyl vinyl ketone have been shown to produce acetylene directly but with varying amounts of internal energy.[17−21] In addition to direct dissociation channels, vinyl radical generated from precursor dissociation may have sufficient energy for dissociation, resulting in significant quantities of highly vibrationally excited acetylene and/or vinylidene, which rapidly isomerizes to ground-state acetylene. Furthermore, the nascent vinyl from precursor dissociation may absorb another 193 nm photon and dissociate, producing vibrationally hot acetylene.[14,15,53] This channel, though, is considered unlikely under the present experimental conditions. There are currently no absorption cross section measurements of the vinyl radical near 193 nm. A strong $\pi^*(2a'') \leftarrow \pi(1a'')$ band, however, has been observed from 225 to 238 nm, with a maximum absorption cross section of $\sim 1 \times 10^{-17}$ cm^2 $molecule^{-1}$.[7] The absorption cross section of the vinyl radical at 193 nm is likely to be more than 1 order of magnitude weaker. The laser fluxes used were typically 30 mJ/cm^2. At this photon flux level, the vinyl generated during the photolysis pulse would, on average, have a dissociation probability of <1%.

VI. Conclusion

Photolysis at 193 nm of five precursor molecules, three of them with deuterated isotopomers, has been used to produce

vibrationally excited vinyl C_2H_3 and vinyl-d_3 C_2D_3. IR emission from the vibrationally excited molecules, predominantly vinyl and acetylene, was recorded by time-resolved Fourier transform emission spectroscopy. The emission spectra were analyzed using two-dimensional cross-spectra correlation analysis for the identification of the bands from the same emitting species. A room-temperature acetylene cell was used to eliminate the bands associated with the fundamental transitions of acetylene which appear in abundance as a photolysis product. Emission bands were identified to be associated with vinyl and vinyl-d_3. Comparison with the anticipated isotope shift of the vibrational frequencies, which can be calculated from ab initio methods, confirms the assignment of the vibrational modes. Altogether, four low-energy bending modes, ν_5 at 1401, ν_6 at 1074, ν_8 at 944, and ν_9 at 897 cm^{-1}, and one stretching mode, ν_4 at 1595 cm^{-1}, of the vinyl-h_3 radical have been assigned. Three bending modes, ν_5 at 1060, ν_6 at 820, and ν_8 at 728 cm^{-1}, of vinyl-d_3 have also been determined. Theoretical calculations are in good agreement, except for the ν_9 mode, which was found to be slightly higher in energy and more intense than calculations predict. Calculated isotopic ratios agree with frequency shifts while sharing the same intensity ratio between vibrational modes. The experimental results here reinforce the low-frequency vinyl-h_3 and vinyl-d_3 results found in absorption measurements in low-temperature noble gas matrixes.

The strongest emission feature near 1300 cm^{-1} appearing in each of the five precursor molecules' spectra is not assigned to vinyl. This feature arises from vibrationally hot acetylene. Vibrationally hot acetylene was produced from the photolysis of VBr, VCl, and 13BD, as expected. It was also observed following dissociation of MVK and VI, which was not previously observed as a primary reaction product. In these cases, it is likely that the vibrationally excited acetylene is produced through another mechanism or secondary dissociation reaction of the vinyl radical and thus warrants further study.

Acknowledgment. This work was supported in part through the U.S. Department of Energy, Basic Energy Sciences, Grant No. DEFG 02-86ER 134584. M.N. and M.J.W. acknowledge support from Temple University. The authors thank Professor Andrew Rappe and Dr. Sarah Mason for helpful discussions.

References and Notes

(1) Letendre, L.; Liu, D.-K.; Pibel, C. D.; Halpern, J. B.; Dai, H.-L. *J. Chem. Phys.* **2000**, *112*, 9209.
(2) Okabe, H. *Photochemistry of Small Molecules*; Wiley: New York, 1978.
(3) Fahr, A.; Laufer, A. H.; Klein, R.; Braun, W. *J. Phys. Chem.* **1991**, *95*, 3218.
(4) Donaldson, D. J.; Okuda, I. V.; Sloan, J. *J. Chem. Phys.* **1995**, *193*, 37.
(5) Hunziker, H. E.; Kneppe, H.; McLean, A. D.; Siegbahn, P.; Wendt, H. R. *Can. J. Chem.* **1983**, *61*, 993.
(6) Blush, J. A.; Chen, P. *J. Phys. Chem.* **1992**, *96*, 4138.
(7) Fahr, A.; Hassanzadeh, P.; Atkinson, D. B. *Chem. Phys.* **1998**, *236*, 43.
(8) Pibel, C. D.; McIlroy, A.; Taatjes, C. A.; Alfred, S.; Patrick, K.; Halpern, J. B. *J. Chem. Phys.* **1999**, *110*, 1841.
(9) Ahmed, M.; Peterka, D. S.; Suits, A. G. *J. Chem. Phys.* **1999**, *110*, 4248.
(10) Xu, K.; Zhang, J. *J. Chem. Phys.* **1999**, *111*, 3783.
(11) Tonokura, K.; Marui, S.; Koshi, M. *Chem. Phys. Lett.* **1999**, *313*, 771.
(12) Osborn, D. L.; Frank, J. H. *Chem. Phys. Lett.* **2001**, *349*, 43.
(13) Pusharsky, M. B.; Mann, A. M.; Yeston, J. S.; Moore, C. B. *J. Chem. Phys.* **2001**, *115*, 10738.
(14) Shahu, M.; Yang, C.-H.; Pibel, C. D.; McIlroy, A.; Taatjes, C. A.; Halpern, J. B. *J. Chem. Phys.* **2002**, *116*, 8343.
(15) Mann, A. M.; Chen, X.; Lozovsky, V. A.; Moore, C. B. *J. Chem. Phys.* **2003**, *118*, 4452.
(16) Wodtke, A. M.; Hintsa, E. J.; Somorjai, J.; Lee, Y. T. *Isr. J. Chem.* **1989**, *29*, 383.
(17) Cao, J. R.; Zhang, J. M.; Zhong, X.; Huang, Y. H.; Fang, W. Q.; Wu, X. J.; Zhu, Q. H. *Chem. Phys.* **1989**, *138*, 377.
(18) Fahr, A.; Braun, W.; Laufer, A. H. *J. Phys. Chem.* **1993**, *97*, 1502.
(19) Blank, D. A.; Sun, W.; Suits, A. G.; Lee, Y. T.; North, S. W.; Hall, G. E. *J. Chem. Phys.* **1998**, *108*, 5414.
(20) Katayanagi, H.; Yonekuira, N.; Suzuki, T. *Chem. Phys.* **1998**, *231*, 345.
(21) Robinson, J. C.; Harris, S. A.; Sun, W.; Sveum, N. E.; Neumark, D. M. *J. Am. Chem. Soc.* **2002**, *124*, 10211.
(22) Robinson, J. C.; Sveum, N. E.; Neumark, D. M. *J. Chem. Phys.* **2003**, *119*, 5311.
(23) Mu, X.; Lu, I.-C.; Lee, S.-H.; Wang, X.; Yang, X. *J. Phys. Chem. A* **2004**, *108*, 11470.
(24) Lee, S.-H.; Chen, W.-K.; Chaudhuri, C.; Huang, W.-J.; Lee, Y. T. *J. Chem. Phys.* **2006**, *125*, 144315/1.
(25) Berkowitz, J.; Mayhew, C. A.; Ruscic, B. *J. Chem. Phys.* **1988**, *88*, 7396.
(26) Riehl, J. F.; Morokuma, K. *J. Chem. Phys.* **1994**, *100*, 8176.
(27) Abrash, S. A.; Zehner, R. W.; Mains, G. J.; Raff, L. M. *J. Phys. Chem.* **1995**, *99*, 2959.
(28) Mains, G. J.; Raff, L. M.; Abrash, S. A. *J. Phys. Chem.* **1995**, *99*, 3532.
(29) Cho, S. H.; Park, W.-H.; Kim, S. K.; Choi, Y. S. *J. Phys. Chem. A* **2000**, *104*, 10482.
(30) Tu, J.; Lin, J. J.; Lee, Y. T.; Yang, X. *J. Chem. Phys.* **2002**, *116*, 6982.
(31) Chang, J.-L. *J. Chem. Phys.* **2005**, *122*, 194321/1.
(32) DeSain, J. D.; Jusinski, L. E.; Taatjes, C. A. *Phys. Chem. Chem. Phys.* **2006**, *8*, 2240.
(33) Kanamori, H.; Endo, Y.; Hirota, E. *J. Chem. Phys.* **1990**, *92*, 197.
(34) Kim, E.; Yamamoto, S. *J. Chem. Phys.* **2002**, *116*, 10713.
(35) Tanaka, K.; Toshimitsu, M.; Harada, K.; Tanaka, T. *J. Chem. Phys.* **2004**, *120*, 3604.
(36) Shepherd, R. A.; Doyle, T. J.; Graham, W. R. *J. Chem. Phys.* **1988**, *89*, 2738.
(37) Tanskanen, H.; Khriachtchev, L.; Rasanen, M.; Feldman, V. I.; Sukhov, F. F.; Orlov, A. Y.; Tyurin, D. A. *J. Chem. Phys.* **2005**, *123*, 064318/1.
(38) Paolucci, D. M.; Gunkelman, K.; McMahon, M. T.; McHugh, J.; Abrash, S. A. *J. Phys. Chem.* **1995**, *99*, 10506.
(39) Forney, J.; Jacox, M. E.; Thompson, W. E. *J. Mol. Spectrosc.* **1995**, *170*, 178.
(40) There have been numerous errors in the labeling of the vibrational modes of the vinyl radical. The correct labeling follows the common notation of highest-symmetry modes labeled highest frequency to lowest frequency, followed by the next highest symmetry, and so on.
(41) Wu, Y.-J.; Lin, M.-Y.; Cheng, B.-M.; Chen, H.-F.; Lee, Y.-P. *J. Chem. Phys.* **2008**, *128*, 204509.
(42) Hartland, G. V.; Xie, W.; Dai, H.-L.; Simon, A.; Anderson, M. J. *Rev. Sci. Instrum.* **1992**, *63*, 3261.
(43) Hartland, G. V.; Qin, D.; Dai, H.-L. *J. Chem. Phys.* **1993**, *98*, 6906.
(44) Hartland, G. V.; Qin, D.; Dai, H.-L. *J. Chem. Phys.* **1997**, *107*, 2890.
(45) Qin, D.; Hartland, G. V.; Dai, H.-L. *J. Phys. Chem. A* **2000**, *104*, 10460.
(46) Letendre, L.; Dai, H.-L. *J. Phys. Chem. A* **2002**, *106*, 12035.
(47) Wilhelm, M. J.; McNavage, W.; Groller, R.; Dai, H.-L. *J. Chem. Phys.* **2008**, *128*, 064313/1.
(48) McNavage, W.; Dailey, W.; Dai, H.-L. *Can. J. Chem.* **2004**, *82*, 925.
(49) Dupuis, M.; Wendoloski, J. J. *J. Chem. Phys.* **1984**, *80*, 5696.
(50) Stanton, J. F.; Bartlett, R. J. *J. Chem. Phys.* **1993**, *98*, 7029.
(51) Stanton, J. F. *Chem. Phys. Lett.* **1995**, *237*, 20.
(52) Wang, J.-H.; Chang, H.-C.; Chen, Y.-T. *Chem. Phys.* **1995**, *206*, 43.
(53) Mebel, A. M.; Chen, Y.-T.; Lin, S.-H. *Chem. Phys. Lett.* **1997**, *275*, 19.
(54) Sattelmeyer, K. W.; Schaefer, H. F., III. *J. Chem. Phys.* **2002**, *117*, 7914.
(55) Dong, F.; Roberts, M.; Nesbitt, D. J. *J. Chem. Phys.* **2007**, 128.
(56) McNavage, W.; Dai, H.-L. *J. Chem. Phys.* **2005**, *123*, 184104/1.
(57) Nikow, M.; Wilhelm, M. J.; Smith, J. M.; Dai, H.-L. To be published.
(58) Orr, B. J. *Int. Rev. Phys. Chem.* **2006**, *25*, 655.
(59) Herman, M. *Mol. Phys.* **2007**, *105*, 2217.
(60) Yamanouchi, K.; Miyawaki, J.; Tsuchiya, S.; Jonas, D. M.; Field, R. W. *Laser Chem.* **1994**, *14*, 183.
(61) Temsamani, M. A.; Herman, M.; Solina, S. A. B.; O'Brien, J. P.; Field, R. W. *J. Chem. Phys.* **1996**, *105*, 11357.
(62) Carvalho, A.; Hancock, G.; Saunders, M. *Phys. Chem. Chem. Phys.* **2006**, *8*, 4337.

(63) Liu, D.-K.; Letendre, L.; Dai, H.-L. *J. Chem. Phys.* **2001**, *115*, 1734.
(64) Abrash, S. A.; Pimentel, G. C. *J. Phys. Chem.* **1989**, *93*, 5828.
(65) Yamashita, S. *Chem. Lett.* **1975**, *9*, 967.
(66) Yamashita, S.; Noguchi, S.; Hayakawa, T. *Bull. Chem. Soc. Jpn.* **1972**, *45*, 659.
(67) Wilhelm, M.; Nikow, M.; Dai, H.-L. *J. Mol. Struct.* **2008**, *242*, 883–884.
(68) Christiansen, O.; Hattig, C.; Jorgensen, P. *Spectrochim. Acta, Part A* **1999**, *55*, 509.
(69) Sattelmeyer, K. W.; Stanton, J. F.; Olsen, J.; Gauss, J. *Chem. Phys. Lett.* **2001**, *347*, 499.
(70) Scott, A. P.; Radom, L. *J. Phys. Chem.* **1996**, *100*, 16502.
(71) Simmonett, A. C.; Evangelista, F. A.; Allen, W. D.; Schaefer, H. F., III. *J. Chem. Phys.* **2007**, 127.
(72) Dong, F.; Davis, S.; Nesbitt, D. J. *J. Phys. Chem. A* **2006**, *110*, 3059.
(73) Curtiss, L. A.; Pople, J. A. *J. Chem. Phys.* **1988**, *88*, 7405.
(74) Galli, C.; Guarnieri, A.; Koch, H.; Mencarelli, P.; Rappaport, Z. *J. Org. Chem.* **1997**, *62*, 4072.
(75) Birss, R. *Comput. Phys. Commun.* **1984**, *38*, 83.
(76) Frisch, M. J.; Trucks, G. W.; Schlegel, H. B.; Scuseria, G. E.; Robb, M. A.; Cheeseman, J. R.; Montgomery, J. A., Jr.; Vreven, T.; Kudin, K. N.; Burant, J. C.; Millam, J. M.; Iyengar, S. S.; Tomasi, J.; Barone, V.; Mennucci, B.; Cossi, M.; Scalmani, G.; Rega, N.; Petersson, G. A.; Nakatsuji, H.; Hada, M.; Ehara, M.; Toyota, K.; Fukuda, R.; Hasegawa, J.; Ishida, M.; Nakajima, T.; Honda, Y.; Kitao, O.; Nakai, H.; Klene, M.; Li, X.; Knox, J. E.; Hratchian, H. P.; Cross, J. B.; Bakken, V.; Adamo, C.; Jaramillo, J.; Gomperts, R.; Stratmann, R. E.; Yazyev, O.; Austin, A. J.; Cammi, R.; Pomelli, C.; Ochterski, J. W.; Ayala, P. Y.; Morokuma, K.; Voth, G. A.; Salvador, P.; Dannenberg, J. J.; Zakrzewski, V. G.; Dapprich, S.; Daniels, A. D.; Strain, M. C.; Farkas, O.; Malick, D. K.; Rabuck, A. D.; Raghavachari, K.; Foresman, J. B.; Ortiz, J. V.; Cui, Q.; Baboul, A. G.; Clifford, S.; Cioslowski, J.; Stefanov, B. B.; Liu, G.; Liashenko, A.; Piskorz, P.; Komaromi, I.; Martin, R. L.; Fox, D. J.; Keith, T.; Al-Laham, M. A.; Peng, C. Y.; Nanayakkara, A.; Challacombe, M.; Gill, P. M. W.; Johnson, B.; Chen, W.; Wong, M. W.; Gonzalez, C.; Pople, J. A. *Gaussian 03*, revision 6.0; Gaussian, Inc.: Pittsburgh, PA, 2003.
(77) The advances presented for the first time in Gaussian 03 are the work of M. J. Frisch, G. W. T., H. B. Schlegel, G. E. Scuseria, M. A. Robb, J. R. Cheeseman, J. A. Montgomery, Jr., T. Vreven, K. N. Kudin, J. C. Burant, J. M. Millam, S. S. Iyengar, J. Tomasi, V. Barone, B. Mennucci, M. Cossi, G. Scalmani, N. Rega, G. A. Petersson, H. Nakatsuji, M. Hada, M. Ehara, K. Toyota, R. Fukuda, J. Hasegawa, M. Ishida, T. Nakajima, Y. Honda, O. Kitao, H. Nakai, M. Klene, X. Li, J. E. Knox, H. P. Hratchian, J. B. Cross, C. Adamo, J. Jaramillo, R. Gomperts, R. E. Stratmann, O. Yazyev, A. J. Austin, R. Cammi, C. Pomelli, J. W. Ochterski, P. Y. Ayala, K. Morokuma, G. A. Voth, P. Salvador, J. J. Dannenberg, V. G. Zakrzewski, A. D. Daniels, O. Farkas, A. D. Rabuck, K. Raghavachari and J. V. Ortiz.
(78) Watson, J. K. G. *J. Chem. Phys.* **1967**, *46*, 1935.
(79) Zou, P.; Strecker, K. E.; Ramirez-Serrano, J.; Jusinski, L. E.; Taatjes, C. A.; Osborn, D. L. *Phys. Chem. Chem. Phys.* **2007**, *10*, 713.
(80) Lin, S.-R.; Lin, S.-C.; Lee, Y.-C.; Chou, Y.-C.; Chen, I.-C.; Lee, Y.-P. *J. Chem. Phys.* **2001**, *114*, 160.
(81) Dong, F.; Roberts, M.; Nesbitt, D. J. *J. Chem. Phys.* **2008**, *128*, 044305.
(82) Herman, M.; Campargue, A.; ElIdrissi, M. I.; Auwera, J. V. *J. Phys. Chem. Ref. Data* **2003**, *32*, 921.

JP809735E